J Mater Sci (2010) 45:188–191
DOI 10.1007/s10853-009-3915-8

Dielectric and piezoelectric properties of $(1 - x)(K_{0.498}Na_{0.498}Li_{0.04})NbO_3$–$x(Bi_{0.5}Na_{0.5})_{0.9}Ba_{0.1}(Zr_{0.0055}Ti_{0.9945})O_3$ lead-free ceramics

Yixiong Liu · Yanqiu Huang · Tiantian Liu ·
Bei Zhang · Qiushi Yan · Guoxi Zhang

Received: 16 July 2009 / Accepted: 19 September 2009 / Published online: 1 October 2009

Abstract $(1 - x)(K_{0.498}Na_{0.498}Li_{0.04})NbO_3$–$x(Bi_{0.5}Na_{0.5})_{0.9}Ba_{0.1}(Zr_{0.0055}Ti_{0.9945})O_3$ (KNLN–BNBZT100x, $x = 0$, 0.01, 0.02, 0.03, 0.05, 0.1) lead-free ceramics were prepared by conventional solid-state reaction technique. The influences of the BNBZT on the crystal structure, dielectric, and piezoelectric properties of the ceramics were investigated. The ceramics formed single-phase solid solutions with perovskite structure after sintering in air at 1050–1100 °C for 3–4 h. Morphotropic phase boundary (MPB) between orthorhombic and tetragonal phase was found in the composition range of $0.01 \leq x \leq 0.02$. The Curie temperature, T_c, and the orthorhombic–tetragonal transition temperature, T_{O-T}, shifted to low temperature as BNBZT increased. The dielectric and piezoelectric properties of ceramics were enhanced for the composition near the MPB. The maximum value, 194 pC/N, of piezoelectric constant d_{33} together with the mechanical quality factor Q_m, 20, were obtained when BNBZT content was 2 mol%.

Introduction

Potassium sodium niobate $(K_{0.5}Na_{0.5})NbO_3$ (KNN) is an attractive lead-free material, which is considered to be the candidate to replace the widely used lead-containing perovskite materials because of its high piezoelectric properties, high Curie temperature, and environmental friendliness [1, 2]. However, it is very difficult to obtain dense KNN ceramics by using an ordinary sintering process because of the high volatility of alkaline elements at high temperature [3, 4]. In order to obtain well-sintered and dense KNN ceramics with good performance, some special sintering methods such as hot pressing and spark plasma sintering techniques [4, 5] and some sintering aids such as CuO, $K_{5.4}Cu_{1.3}Ta_{10}O_{29}$, $K_4CuNb_8O_{23}$, and GeO_2 [6–9] were used. Some other ABO_3 perovskites were also used to form solid solutions with KNN [10–13]. Previous studies showed that the modified KNN ceramics, obtained by using Li, Ta, and Sb to replace the A and/or the B site cation of the ABO_3 perovskite structure, exhibited good piezoelectric properties [2, 14, 15]. The solid solution ceramics of KNN with $BaTiO_3$ (BT), $(Bi_{0.5}Na_{0.5})TiO_3$ (BNT), or $Ba(Ti,Zr)O_3$ (BZT) also exhibited good dielectric and piezoelectric properties [13, 16, 17]. However, few reports are involved with the solid solutions formed in $(K_{0.5}Na_{0.5})NbO_3$–$LiNbO_3$–$(Bi_{0.5}Na_{0.5})TiO_3$–$Ba(Ti,Zr)O_3$ system.

The purposes of the present study are to investigate the effect of BNT–BZT content on the properties of KNN-based solid solution ceramics. In this work, $(1 - x)(K_{0.498}Na_{0.498}Li_{0.04})NbO_3$–$x(Bi_{0.5}Na_{0.5})_{0.9}Ba_{0.1}(Zr_{0.0055}Ti_{0.9945})O_3$ (abbreviated as KNLN–BNBZT100x) solid solution ceramics were prepared by normal sintering. The effects of the $(Bi_{0.5}Na_{0.5})_{0.9}Ba_{0.1}(Zr_{0.0055}Ti_{0.9945})O_3$ (BNBZT) on the phase structure, dielectric, ferroelectric, and piezoelectric properties of the ceramics were investigated.

Experiment

The KNLN–BNBZT100x ($x = 0$, 0.01, 0.02, 0.03, 0.05, 0.1) ceramics were prepared by conventional solid-state

Y. Liu · Y. Huang (✉) · T. Liu · B. Zhang · Q. Yan · G. Zhang
Engineering Research Center of Nano-Geomaterials of Ministry of Education, China University of Geosciences, Wuhan 430074, People's Republic of China
e-mail: y.q.huang@163.com

Y. Liu · Y. Huang · T. Liu · B. Zhang · Q. Yan · G. Zhang
Faculty of Materials Science and Chemical Engineering, China University of Geosciences, Wuhan 430074, People's Republic of China

reaction technique. The starting raw materials were reagent grade K_2CO_3, Na_2CO_3, Li_2CO_3, $BaCO_3$, Bi_2O_3, TiO_2, Nb_2O_5, and $Zr(NO_3)_4 \cdot 5H_2O$. The powders were mixed in stoichiometric proportions and milled in ethanol for 12 h, then dried and calcined at 850 °C for 5 h. The calcined powders were reground and then pressed into discs with 20 mm in diameter and about 1–1.5 mm in thickness. The green discs were finally sintered in air at 1050–1100 °C for 3–4 h. Electrodes were made on the surfaces of the discs by firing silver paste at 600 °C for 10 min. The electric poling was performed under a dc field of 2 kV/mm at 110 °C in a silicone oil bath for 15 min.

The crystal structure of the sintered samples was determined by using an X-ray diffractometer (X′ Pert PRO) with a Cu Kα radiation. Dielectric measurements were carried out by a TH2819 Precision LCR Meter at 10 kHz from room temperature to 450 °C. The coercive field, E_c, and remanent polarization, P_r, were determined from the hysteresis loops obtained by the modified Sawyer-Tower circuit. The piezoelectric constant d_{33} was measured by a ZJ-A3 quasi-static piezoelectric d_{33} meter. The electromechanical coupling factors, k_p and k_t, were determined by a resonance–antiresonance method with an impedance analyzer (HP4294A).

Results and discussion

Figure 1 shows the X-ray diffraction (XRD) patterns of the KNLN–BNBZT100*x* ceramics with 0, 1, 2, 3, and 5 mol% BNBZT. It is found that all the ceramics form single-phase solid solutions with perovskite structure. The solid solutions are of orthorhombic symmetry when BNBZT content is 0–1 mol% (the corresponding XRD patterns can be indexed in JCPDS-ICDD 71-2171). As BNBZT content increases, a tetragonal phase appears. When BNBZT content reaches 2 mol%, the ceramic possesses the tetragonal phase only (the corresponding XRD patterns can be indexed in JCPDS-ICDD 71-0945). These suggest that the system has an orthorhombic–tetragonal morphotropic phase boundary (MPB) at $x = 0.01$–0.02.

Figure 2 shows the temperature dependence of the relative permittivity, ε_r, and loss tangent, tanδ, of the KNLN–BNBZT100*x* ceramics at 10 kHz. The phase transitions for the KNLN ceramic are observed at 441 and 146 °C, corresponding to the transition temperatures (T_c and T_{O-T}) from the tetragonal phase to the cubic phase and from the orthorhombic phase to the tetragonal phase, respectively. The Curie temperature (T_c) is a little higher than that of the pure KNN, but the orthorhombic–tetragonal transition temperature (T_{O-T}) is obviously lower than that of the pure KNN. As BNBZT increases, both T_c and T_{O-T} shift to lower temperature. When BNBZT content is ≥2 mol%, only the cubic–tetragonal phase transition is observed, indicating that the structure of the solid solutions had changed from orthorhombic to tetragonal at room temperature. This result is consistent with XRD analysis as discussed in Fig. 1. When BNBZT content is ≥5 mol%, the dielectric peaks of the ceramics at T_c become much lower and broad. These phenomena may be attributed to the more complex occupation of the A and B sites in an ABO_3 perovskite structure and heterogeneous compositions [18, 19]. For all samples, a broad peak near the room temperature can be observed in both the ε_r–*T* curves and the tanδ–*T* curves. The peak

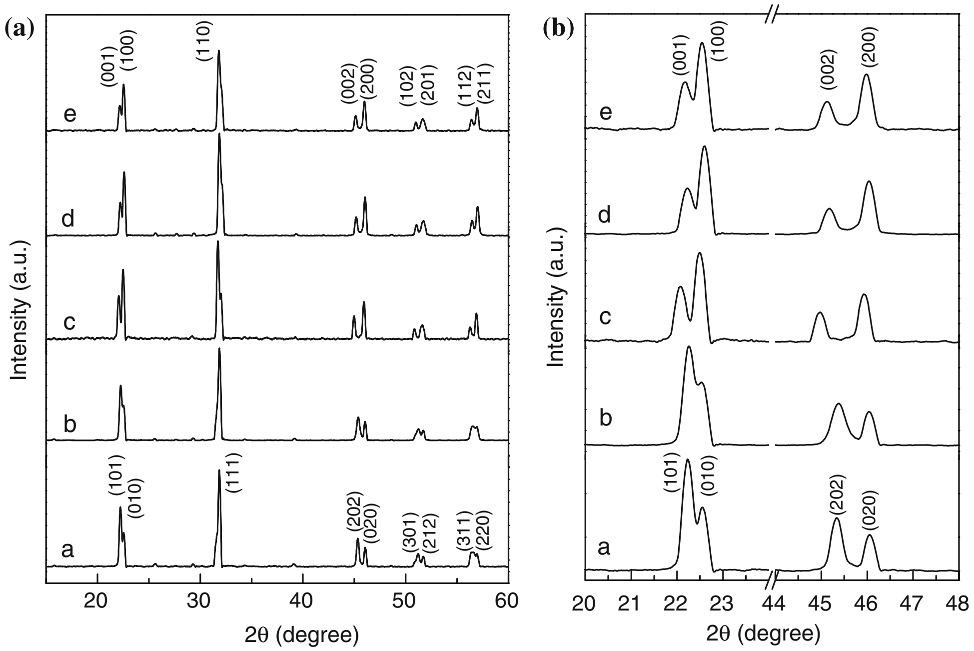

Fig. 1 XRD patterns of KNLN–BNBZT100*x* ceramics of *a* KNLN, *b* KNLN–BNBZT1, *c* KNLN–BNBZT2, *d* KNLN–BNBZT3, *e* KNLN–BNBZT5. **a** Wide range and **b** selected portions

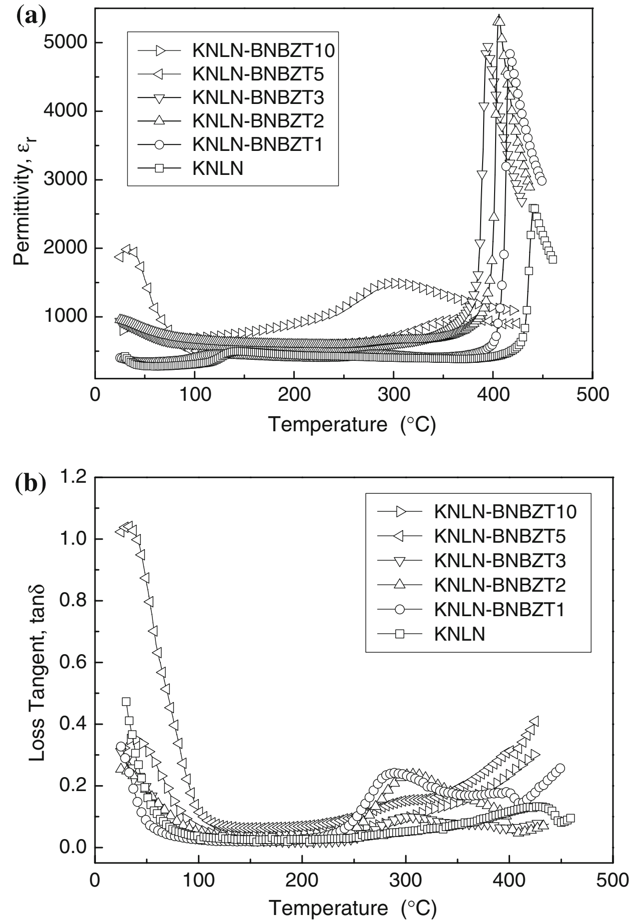

Fig. 2 Temperature dependence of **a** permittivity and **b** loss tangent of the ceramics with different BNBZT content at 10 kHz

becomes strong as BNBZT content increases, especially when BNBZT content is 5 mol%. These characteristics indicate that an intermediate phase transition took place near the room temperature, and BNBZT can affect the phase transition to some extent.

Figure 3 shows the tendency of the dielectric constant $\varepsilon_{33}^{T}/\varepsilon_0$ and the dissipation factor tanδ of the poled ceramics with the content of BNBZT. The $\varepsilon_{33}^{T}/\varepsilon_0$ of ceramics with 1–3 mol% BNBZT increases obviously from 460 to 1630, indicating that the dielectric properties may be enhanced for compositions near the MPB. When BNBZT content is higher than 3 mol%, the $\varepsilon_{33}^{T}/\varepsilon_0$ of the ceramics decreases slightly with further increasing BNBZT. The tanδ of the ceramics decreases with the increase of BNBZT when BNBZT content is 0–3 mol%, but increases rapidly thereafter with further increase in BNBZT.

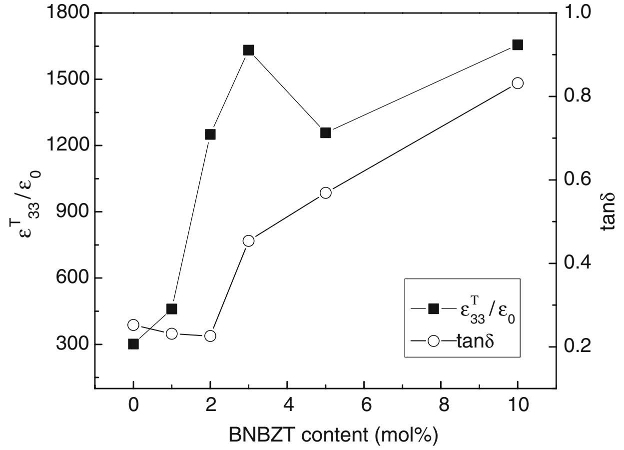

Fig. 3 Dielectric constant, $\varepsilon_{33}^{T}/\varepsilon_0$, and the dissipation factor, tanδ versus the BNBZT content for the KNLN–BNBZT100x ceramics

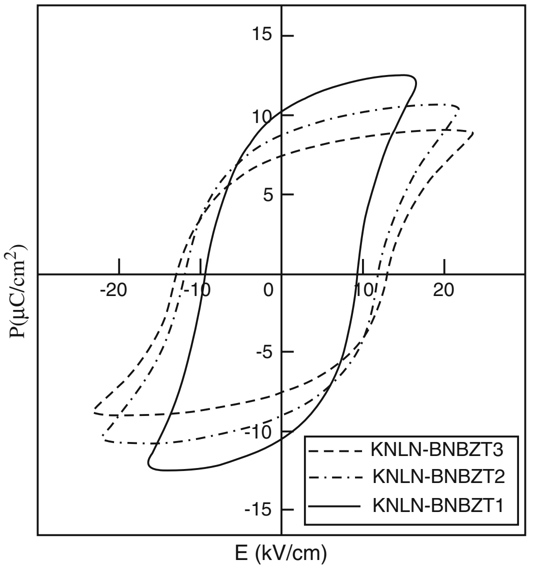

Fig. 4 *P–E* hysteresis loops of the KNLN–BNBZT100x ceramics at room temperature

Figure 4 shows the *P–E* hysteresis loops of the KNLN–BNBZT100x ($x = 0.01$, 0.02, 0.03) ceramics at room temperature. The shape of the loops and the value of polarization are influenced significantly by BNBZT content. The values of the remanent polarization, P_r, are 10.3, 8.7, 7.1 μC/cm^2 when BNBZT content is 1, 2, 3 mol%, respectively. Whereas the coercive field, E_c, of the ceramics with 1, 2, 3 mol% BNBZT is 9.3, 12, 13.3 kV/cm, respectively, increasing monotonously as BNBZT increases. These characteristics indicate that the domain reorientation and rotation will be gradually hindered as BNBZT increases.

Figure 5 shows the piezoelectric constant, d_{33}, and the mechanical quality factor, Q_m, of the ceramics as a function of the BNBZT content. It is found that the d_{33} enhances for compositions near the MPB. The maximum value, 194 pC/N, of the d_{33} is obtained in the composition of 2 mol% BNBZT. As the BNBZT content increases further, the d_{33} decreases gradually. The unique properties of the ceramics are that the mechanical quality factor Q_m is

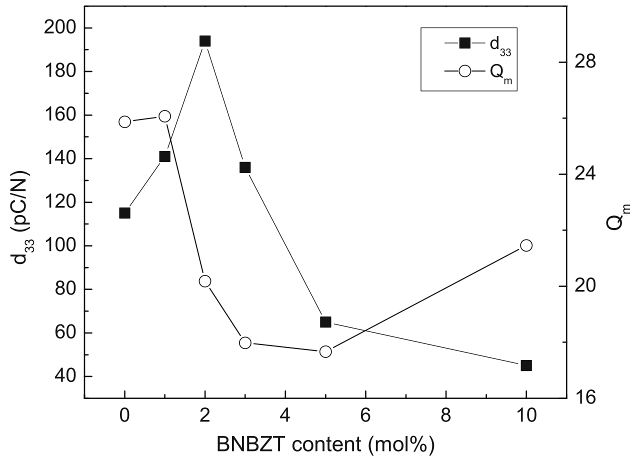

Fig. 5 Piezoelectric constant, d_{33}, and mechanical quality factor, Q_m, versus the BNBZT content for the KNLN–BNBZT100x ceramics

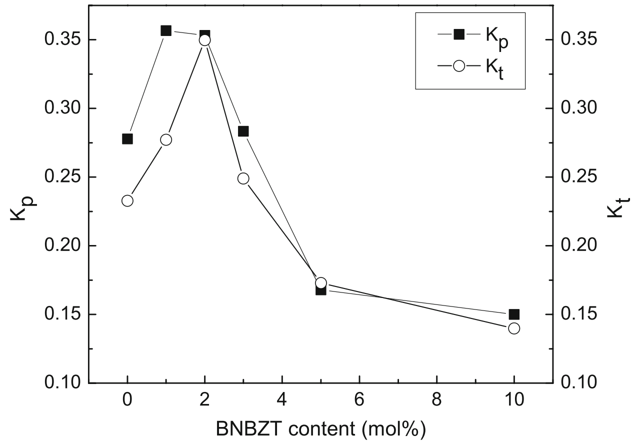

Fig. 6 Electromechanical coupling factors, k_p and k_t, versus the BNBZT content for the KNLN–BNBZT100x ceramics

very low ($Q_m \leq 26$). As BNBZT content increases, the Q_m decreases. The lowest value, 17.7, of Q_m is obtained when BNBZT content is 5 mol%. These properties correspond to that of $PbNb_2O_6$-based piezoelectric ceramics, which were found to have a very low Q_m and were considered to be used for wide band ultrasonic transducers [20, 21].

Figure 6 shows the electromechanical coupling factors, k_p and k_t, of the ceramics as a function of BNBZT content. It can be found that both of k_p and k_t reach a maximum value when the composition is near the MPB. When BNBZT content is higher than 2 mol%, both of k_p and k_t decrease with the increase of BNBZT. These characteristics indicate that the MPB plays an important role in improving piezoelectric properties of KNLN–BNBZT ceramics.

Conclusion

The influences of the BNBZT on the crystal structure, dielectric, ferroelectric, and piezoelectric properties of the KNLN–BNBZT100x ($x = 0$, 0.01, 0.02, 0.03, 0.05, 0.1) ceramics have been studied. XRD analysis revealed that there was a MPB between orthorhombic and tetragonal phases at $x = 0.01$–0.02. The Curie temperature, T_c, and the orthorhombic–tetragonal transition temperature, T_{O-T}, decreased as BNBZT increased. The ceramics had a very low mechanical quality factor Q_m, which decreased as BNBZT increased. The dielectric and piezoelectric properties of ceramics were enhanced for the composition near the MPB. The maximum value, 194 pC/N, of piezoelectric constant d_{33} together with the mechanical quality factor Q_m, 20, were obtained when BNBZT content was 2 mol%.

Acknowledgements The authors are grateful to Mr. Jishun Yu for XRD analysis and Ms. Michun Yang for assistance in performing the dielectric and piezoelectric property measurements.

References

1. Egerton L, Dillon DM (1959) J Am Ceram Soc 42:438
2. Saito Y, Takao H, Tani T, Nonoyama T, Takatori K, Homma T, Nagaya T, Nakamura M (2004) Nature 432:84
3. Shirane G, Newnham R, Pepinsky R (1954) Phys Rev 96:581
4. Jaeger RE, Egerton L (1962) J Am Ceram Soc 45:209
5. Wang RP, Xie RJ, Sekiya T, Shimojo Y (2004) Mater Res Bull 39:1709
6. Lin DM, Kwok KW, Chan HLW (2008) J Phys D Appl Phys 41:045401
7. Lin DM, Kwok KW, Chan HLW (2008) J Appl Phys 103:064105
8. Matsubara M, Yamaguchi T, Kikuta K, Hirano S (2004) Jpn J Appl Phys 43:7159
9. Bernard J, Bencan A, Rojac T, Holc J, Malic B, Kosec M (2008) J Am Ceram Soc 91:2409
10. Guo Y, Kakimoto K, Ohsato H (2004) Appl Phys Lett 85:4121
11. Du HL, Tang FS, Liu DJ, Zhu DM, Zhou WC, Qu SB (2007) Mater Sci Eng B 136:165
12. Zang GZ, Wang JF, Chen HC, Su WB, Wang CM, Qi P, Ming BQ, Du J, Zheng LM, Zhang SJ, Shrout TR (2006) Appl Phys Lett 88:212908
13. Ahn CW, Choi CH, Park HY, Nahm S, Priya S (2008) J Mater Sci 43:6784. doi:10.1007/s10853-008-2934-1
14. Hollenstein E, Davis M, Damjanovic D, Setter N (2005) Appl Phys Lett 87:182905
15. Hao JG, Chu RQ, Xu ZJ, Zang GZ, Li GR (2009) J Alloy Comp 479:376
16. Zuo RZ, Ye C (2007) Appl Phys Lett 91:062916
17. Lin DM, Kwok KW, Chan HLW (2007) Appl Phys Lett 91: 143513
18. Huang CC, Cann DP, Tan X, Vittayakorn N (2007) J Appl Phys 102:044103
19. Sutapun M, Huang CC, Cann DP, Vittayakorn N (2009) J Alloy Comp 479:462
20. Soejima J, Nagata K (2001) Jpn J Appl Phys 40:5747
21. Nagata K, Soejima J (2002) Ferroelectrics 273:77